になる。

今後、このような試料を用いてプロセスバリデーションのモデル実験を進める一方、界面活性剤を含まないスパイク用試料の調整法についても検討する必要があると思われる。

E. 結論

粒子径の小さい PrP^{Sc} を大量に回収することは困難であるが、本研究では、PrP^{Sc} 検出感度に優れた PMCA を検出に用いることで、粒子径 35 nm 以下の PrP^{Sc} 画分をスパイク用試料として用いた場合でも、10^3ー10^4 のレンジでのプロセスバリデーションが実施可能であることを示した。今後、粒子径の小さい PrP^{Sc} を用いることで、より厳密に医薬品の製造工程における PrP^{Sc} 除去効率が評価できるようになると思われる。

F. 健康危険情報

実験室内感染、外部への病原体の拡散などの事故は発生していない。

G. 研究発表

1. 論文発表

1) Song C-H, Furuoka H, Kim C-L, Ogino M, Suzuki A, Hasebe R, and Horiuchi, M. Intraventricular infusion of anti-PrP mAb antagonized PrP^{Sc} accumulation and delayed disease progression in prion-infected mice. J. Gen. Virol. 2008: 89;1533-1544.
2) Muramatsu Y, Sakemi Y, Horiuchi M, Ogawa T, Suzuki K, Kanameda M, Tran Thi Hanh TT, and Tamura Y. Frequencies of PRNP gene polymorphisms in Vietnamese dairy cattle for potential association with BSE. Zoonoses Public Health. 2008: 55; 267-273.
3) Takada N, Horiuchi M, Sata T, and Sawada Y. Evaluation of methods for removing central nervous system tissue contamination from the surface of beef carcasses after splitting. J. Vet. Med. Sci. 2008: 70; 1225-1230.
4) Watanabe K, Tachibana M, Tanaka S, Furuoka H, Horiuchi M, Suzuki H, and Watarai M. Heat shock cognate protein 70 contribute Brucella invasion into trophoblast giant cells that cacuse infectious abortion. BMC Microbiol. 2008: 8; 212.
5) Shindoh R, Kim C-L, Song C-H, Hasebe R, and Horiuchi M. The region approximately between amino acids 81 and 137 of proteinase K-resistant PrP^{Sc} is critical for the infectivity of the Chandler prion strain. J. Virol. in press.
6) 堀内 基広. プリオンの増殖とその抑制. ウイルス感染症セミナー. 2008:10;13-25.

2. 学会発表

1) Song C-H, Honmou O, Furuoka H, Hasebe R, and Horiuchi M. Migration of mesenchymal stem cells to brain lesions of prion disease. Prion2008 (Sept. 26-28, 2008, Madrid, Spain)
2) Furuoka H, Horiuchi M, and Sata T. Pathology in guinea pig infected with bovine spongiform encephalopathy. Prion2008 (Sept. 26-28, 2008, Madrid, Spain)
3) Shindo R, Kim C-L, Song C-H Hasebe R., and Horiuchi M. Conformational stability and

infectivity of protease-resistant prion protein derived from the Chandler strain. Prion2008 (Sept. 26-28, 2008, Madrid, Spain)

4) Yamasaki T, Uryu M, Nakamitsu S, and Horiuchi M. Localization of disease-specific prion protein in prion-infected cells. Asian-African Research forum on Emergig and Reemerging Infection. (Dec. 15-16, 2008, Sapporo, Japan)
5) Horiuchi M and Yamazaki T. Intracellular Localization of Disease-Specific Prion Protein. Symposium on emerging and reemerging infectious diseases (Feb. 17, 2009, Yokyo)
6) 前野英毅、村井活史、武田芳於、鬼塚剛志、脇坂明美、沼田芳彰、堀内基広. ウイルス除去膜濾過による異常型プリオン蛋白質(PrP^{Sc})の除去. プリオン研究会 2008 (2008年8月29-30日, 新得)
7) 宋昌鉉、本望修、古岡秀文、長谷部理絵、堀内基広. プリオン感染マウス脳における骨髄由来間葉系幹細胞の動態. プリオン研究会 2008 (2008年8月29-30日, 新得)
8) 山崎剛士、瓜生匡秀、中満智史、堀内基広. 間接蛍光抗体法によるプリオン持続感染細胞に存在するPrPSc の検出. プリオン研究会 2008 (2008年8月29-30日, 新得)
9) 鈴木章夫、山崎剛士、堀内基広 PrP-Fc融合蛋白質とPrPScの結合条件の検討. プリオン研究会 2008 (2008年8月29-30日, 新得)
10) 堀内 基広、瓜生 匡秀、山崎 剛士、中満 智史、長谷部 理絵. マウス神経芽腫細胞 Neuro2a におけるプリオンの細胞間伝播にはエクソソーム以外の因子が関与する. 第146回日本獣医学会 (2008年9月24-26日, 宮崎)
11) 宋昌鉉、長谷部理絵、堀内基広. プリオン感染マウス脳における骨髄由来間葉系幹細胞の動態. 第56回日本ウイルス学会 (2008年10月26-28日, 岡山)
12) 山崎剛士、瓜生匡秀、中満智史、堀内基広. 間接蛍光抗体法によるプリオン持続感染細胞に存在するPrPScの検出. 第56回日本ウイルス学会 (2008年10月26-28日, 岡山)
13) 堀内基広、長谷部理絵. PrPScのaa 81 - aa 137の領域はプリオンの感染性に必須である. 第56回日本ウイルス学会 (2008年10月26-28日, 岡山)

H. 知的財産権の出願・登録状況（予定を含む）

1. 特許取得

本年度は該当なし。

2. 実用新案登録

本年度は該当なし。

3. その他

本年度は該当なし

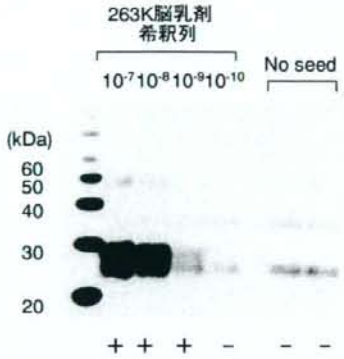

図１．PMCA の結果の判定。

プリオン非感染ハムスターの脳乳剤を同様の条件で PMCA を実施した場合、典型的な PrP^{Sc} 由来のバントよりも分子量が小さいバンドが検出される場合がある(No seed)。このようなバンドが検出された場合、およびバンドが検出されなかった場合を陰性と判定した。+は陽性と判定したバンドを示す。

表１．各 PrP^{Sc} 画分の $PMCA_{50}$ 値

PrP^{Sc} 画分	希釈列							PrP^{Sc} 濃度
	10^{-4}	10^{-5}	10^{-6}	10^{-7}	10^{-8}	10^{-9}	10^{-10}	Log[$PMCA_{50}$/mL]
スパイク用試料	NT	NT	+++[b]	+++	+--[c]	---[d]	---	11.3
プラノバ 20N 濾液	++[a]	++	+++	---	---	NT	NT	9.9
プラノバ 15N 濾液	+++	+++	---	---	---	NT	NT	8.9

a) n = 2で実施し、2検体ともにPrP^{Sc}陽性であったことを示す。
b) n = 3で実施し、3検体ともにPrP^{Sc}陽性であったことを示す。
c) n = 3で実施し、1検体のみPrP^{Sc}陽性であったことを示す。
d) n = 3で実施し、3検体ともPrP^{Sc}が増幅されなかったことを示す。

表２．SUS 濃度がスパイク用試料の PrP^{Sc} 力価に及ぼす影響

PrP^{Sc} 画分	希釈列							PrP^{Sc} 濃度
	10^{-1}	10^{-2}	10^{-3}	10^{-4}	10^{-5}	10^{-6}	10^{-7}	Log[$PMCA_{50}$/mL]
濾過前 a)	NT	NT	+++	+++	++−	−−−	−−−	8.6
プラノバ 35N 濾液	+	+++	+++	−−−	−−−	NT	NT	6.9

a) 表1のスパイク用試料をPBSで100倍に希釈した。

厚生労働科学研究費補助金（医薬品・医療機器等レギュラトリーサイエンス総合研究事業）
平成20年度分担研究報告書

遺伝子組換え医薬品等のプリオン安全性確保のための検出手法の標準化及びプリオン除去工程評価への適用に関する研究

-異常型プリオンの新規検出法に関する試験研究-

研究分担者　国立医薬品食品衛生研究所　衛生微生物部　菊池裕

研究要旨

遺伝子組換え医薬品等の安全性を確保するため、その原材料に混入する恐れがあるウシ異常型プリオン蛋白質(PrP^{Sc})の高感度な検出法の開発が望まれている。動物由来製造原材料の品質確保および種々の製造工程の安全性評価を目的としたPrP^{Sc}の検出法の開発に資する基礎研究として、ウシスプライス変異型プリオン蛋白質(PrPSV)標準品の確保を目的とした大腸菌による発現系の構築、RT-PCR法によるウシ血液中のPrPSVの検出およびヒツジPrPSV mRNAの探索を行った。

大腸菌によるウシプリオン蛋白質(PrP)及びPrPSVの産生は、それぞれの遺伝子を導入した大腸菌溶解液をSDS-PAGEで泳動し、市販の抗PrPモノクローナル抗体6H4を用いたイムノブロット法を行い、その発現を確認した。得られたPrPSVを用い、抗PrPSVモノクローナル抗体産生ハイブリドーマ樹立を試みている。

プリオン病のバイオマーカーへの適用を目的としたウシ血液中のPrPSV mRNAの検出は、全血から調製したtotal RNAを用いたRT-PCR法を行い、PrPSV mRNAの発現を確認した。しかし、その発現量は低く、定量RT-PCR法では検出できなかった。

ヒツジPrPSV mRNAの探索にはヒツジ脳由来total RNAからcDNAを調製し、各種プライマーを用いて産生したPCR産物の塩基配列を解析し、ヒツジPrPのGPIアンカーシグナルペプチドを欠損したPrPSV mRNAをクローニングした。このmRNA由来fs-cDNAを特異的に増幅するexon-exon junction primerを用いたRT-PCRを構築した。これらの研究成果は、スクレイピーやBSE罹患ヒツジ試料を用いた解析等への応用が期待される。

A. 研究目的

人のプリオン病には硬膜移植等によって発症した感染性CJD、プリオン蛋白質遺伝子(*PRNP*)にコードされた253残基のアミノ酸に変異がある遺伝型CJD及び*PRNP*に変異のない散発型CJDが知られ、約85-90%を散発性CJDが占めている。一方、1996年に英国で発症が確認された変異型CJDは、従来の散発型CJDとは異なって若年性の患者で発症し、異常型プリオン蛋白質(PrP^{Sc})の生化学的研究及び英国で多発していた牛海綿状脳症(BSE)に関する疫学研究から、ウシPrP^{Sc}の人への伝達によって発症すると考えられている。また、輸血によって変異型CJDを発症したと推定される症例が報告されており、血液を介したCJDの伝達が注目を集めている。多くの遺伝子組換え医薬品等の製造工程ではウシ胎児血清を用いることから、医薬品へのPrP^{Sc}汚染を防ぐために、ウシ由来原材料中のPrP^{Sc}測定法の確立が望まれている。

昨年の本研究ではウシ角膜細胞株BCE C/D-1b及びウシ脳から調製したtotal RNAを用い、プリオン蛋白質(PrP)のGPIアンカーシグナルペプチドを欠損したスプライス変異型プリオン蛋白質(PrPSV) mRNAの発現について報告した。ウシPrPは264残基のアミノ酸配列を有し、242-264残基はGPIアンカーシグナル配列と推定され、241残基のAlaを介して細胞膜上に結合している。一方、ウシPrPSV mRNAから推定されるアミノ酸配列は260残基からなり、1-240残基はPrPと共通で、C末端の241-260残基は異なったアミノ酸配列を有している。

本年度は、大腸菌を用いたウシPrPSV発現系の構築、ウシ血液から調製したtotal RNAを用いたPrPSV mRNAの検出及びヒツジPrPSV mRNAの同定を行った。

B. 研究方法

1. 細胞培養

ヒツジ胎児脳由来細胞株OA1 (ATCC Number: CRL-6538)はT75組織培養用フラスコで培養し、1週間に1度の継代を行った。長期間の培養は9-cm組織培養用シャーレで行い、4日ごとに培地を交換した。

2. ウシ血液

血液は北海道畜産試験場で正常ウシから採血し、3倍量のRNAlater (Ambion)を加え、使用時まで-20°C下に保存した。

3. RT-PCR

培養したOA1細胞又は血液からDNase I消化したtotal RNAを調製し、スーパースクリプトIII RNase H-逆転写酵素(インビトロジェン株式会社)を用いてfs-cDNAを合成し、RT-PCRに用いた。同時にゲノムDNAを調製し、陽性対象としてPCRに用いた。PCRはウシ又はヒツジ*PRNP*のエクソン3にコードされているオープンリーディングフレーム(ORF)のmRNAを検出する各種プライマーと、Ex taq polymerase (タカラバイオ株式会社)を用いて行った。

4. ウシPrPSVの発現

ウシPrP又はPrPSV遺伝子エクソン3のORFを組み込んだpET-22bベクターを*Escherichia coli* BL21(DE3)pLysSに導入し、Overnight Express Autoinduction System I (Novagen)を用いて発現を誘導した。

5. イムノブロット法

試料をSDS-PAGEで分離後にPVDF膜へ転写し、第1抗体として抗PrP抗体6H4 (ロシュ・ダイアグノスティックス株式会社)を、第2抗体にHRP標識抗IgG抗体を用いたイムノブロッティングを行い、コニカイムノステインHRP-1000 (生化学バイオビジネス株式会社)で検出した。

(倫理面への配慮)

本研究の遂行にあたり、「ヒトゲノム・遺伝子解析研究に関する倫理指針」、「国立医薬品食品衛生研究所研究倫理審査委員会規定」、「同病原体等安全管理規程」、「同動物実験に関する指針」及び「同遺伝子組換え実験安全管理規則」を遵守した。

C. 研究結果

1. ウシPrPSV発現系の構築

大腸菌の蛋白質発現系を用い、ウシ角膜細胞株BCE C/D-1bからクローニングしたPrPSV遺伝子を導入し、イムノブロット法でPrPSVの産生を調べた(Fig. 1)。ウシPrP遺伝子を導入した全細胞溶解液では、25 kDa付近に抗PrPモノクローナル抗体6H4が認識するバンドを検出した(Fig. 1. lower panel、lane 1)。同様に、ウシPrPSV遺伝子を導入した全細胞溶解液では、6H4が認識する25 kDaのバンドを検出した(Fig. 1. lower panel、lane 2)。構築した発現系は、6H4抗体が認識するPrPSVを産生することが確認された。

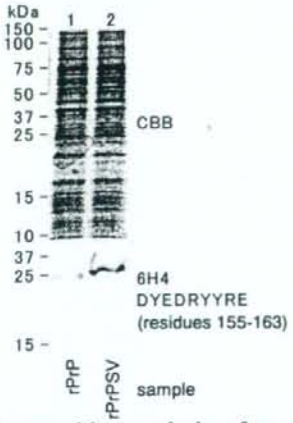

Fig. 1. Immunoblot analysis of recombinant bovine PrP and its splice variant.
The bovine PrP gene and splice variant were subcloned into and transformed into *Escherichia coli* BL21(DE3)pLysS. Cell lysates were subjected to SDS-PAGE and visualized with CBB stain (upper panel). Recombinant PrP and PrPSV were detected with anti-PrP mAb 6H4 (lower panel). Epitope recognition site located within PrP and PrPSV is shown as residues number.

2. ウシ血液中からPrPSV mRNAの検出

ウシ血液からtotal RNAを調製し、exon-exon junction primerを用いたRT-PCR法でPrPSV mRNAの産生を調べた。RNAlater中で長期間保存していたウシ血液の白血球を含む画分からvanadyl ribonucleoside complexを用いてtotal RNAを調製し、同じ画分から定法にしたがってゲノムDNAを調製した。PrP全長を検出するプライマー(BoE3U1/BoE3L7)ではゲノムDNA及びtotal RNAから調製したcDANでは1,347 bpのバンドを示し(Fig. 2、lanes 3 and 7)、コントロールとして用いたPrPSV遺伝子を含むプラスミドでは511 bpを欠失した836 bpのバンドが検出された(Fig. 2、lane11)。PrPSVを特異的に検出するexon-exon junction primer (BoE3SV5/BoE3L4)ではプラスミドと同様な130 bpのバンドがわずかながらcDNAで検出されたが(Fig. 2、lanes 5 and 9)、ゲノムDNAでは検出されなかった(Fig. 2、lane 1)。しかし、744 bpのバンドを検出するexon-exon junction primer (BoE3U1/BoE3SV6)では、cDNAでバンドは検出されなかった(Fig. 2、lanes 6 and 10)。

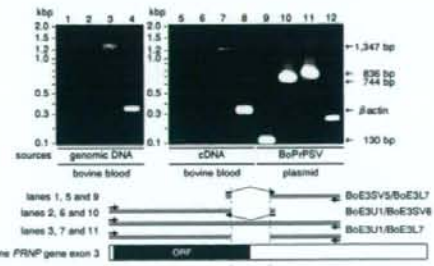

Fig. 2. Detection of the splice variant of PrP mRNA using exon-exon junction primers in total RNA from bovine blood.
We prepared genomic DNA and first-strand cDNA from total RNA from bovine blood and subjected it

to PCR using exon–exon junction (lanes 2, 6 and 10, BoE3U1/BoE3SV6; lanes 1, 5 and 9; BoE3SV5/BoE3L7) and bovine *PRNP* exon 3 (lanes 3, 7 and 11, BoE3U1/BoE3L7), and β-actin primer sets using Ex Taq DNA polymerase. PCR products were separated on a 2% agarose gel and visualized with ethidium bromide.

Fig. 3. Expression of the splice variant of PrP mRNA.

(A) First-strand cDNA from total RNA from sheep brain (5 μg) and genomic DNA from sheep skeletal muscle were used for PCR using sheep *PRNP* exon 3 primers (BoE3U1/BoE3L7, lanes 1 and 2; SE3U0/BoE3L7, lanes 2 and 4) and β-actin primers (lanes 3 and 6) with Ex taq polymerase. PCR products were separated on a 2% agarose gel and visualized with ethidium bromide.

(B) OA1 cells were cultured for 40 days after 5 passages (P5D40). First-strand cDNA and genomic DNA from OA1 cells (left panel) were prepared. First-strand cDNA from sheep brain and genomic DNA from sheep skeletal muscle (right panel) were prepared. First-strand cDNA from total RNA (5 μg) and genomic DNA (2.5 ng) were used for PCR using PrP primer set (P), exon-exon junction primer sets (J1 and J2) and β-actin primers (A) with Ex Taq DNA polymerase. PCR products were separated on a 2% agarose gel and visualized with ethidium bromide.

(C) We confirmed the sequences of ordinary (upper panel) and alternatively spliced sheep *PRNP* (lower panel). Cryptic donor and acceptor sites are designated as exon 3a and 3b, respectively. The untranslated regions (white bars), ORFs (black bars), retained intron (double line), additional ORF (gray bar), and deduced amino acid sequences of ordinary and alternatively spliced (underlined) *PRNP* are indicated. The arrow indicates a GPI anchoring site.

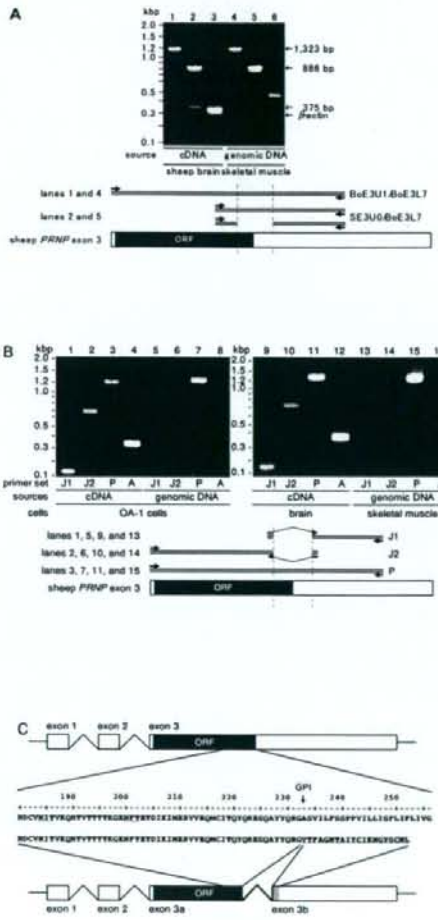

3. ヒツジスプライス変異型プリオン蛋白質mRNAの解析

ヒツジPrP mRNAの発現様式を調べるため、市販のヒツジ脳から調製したtotal RNA (Zyagen Laboratories)から合成したfs-cDNAを鋳型としたRT-PCRを行った。cDNAを測定したRT-PCR法では、PrPに相当する1,323 bpと886 bpのバンドの他に、発現量は少ないが375 bpのバンドを検出した(Fig. 3A, lanes 1 and 2)。それぞれのバンドをゲルから切り出して塩基配列を解析したところ、1,323 bpの塩基配列はORFを含むヒツジ*PRNP*遺伝子エクソン3をコードし、886 bpの塩基配列ではPrPのC末端に位置するGPIアンカーシグナル配列を含む511 bpが欠落していた(Fig. 3C)。一方、ヒツジ骨格筋から調製したゲノムDNAを測定したPCR法では全長1,323 bpのPrPに相当するバンドを示し(Fig. 3A、lane 4)、その塩基配列はtotal RNA由来の1,323 bpのバンドと一致したが、886 bpのバンドは検出されなかった(Fig. 3A, lane 5)。以上の結果から、ヒツジ脳では*PRNP*遺伝子エクソン3のスプライス変異型mRNAを発現することが示唆された。

次に、エクソン結合部位に結合するプライマー(exon-exon junction primer)を設計し、スプライス変異型PrPのmRNAを特異的に検出するRT-PCRを構築した。スプライシングで欠落する部位(511 bp)を挟み、その両端の配列を結合させたプライマーを用いたPCRは、fs-cDNAに130及び716 bpのバンドを示したが(Fig. 3B、lanes 9-10)、genomic DNAではバンドが検出されなかった(Fig. 3B、lanes 13-14)。また、切り出した130及び716 bpのバンドの塩基配列は、エクソン3の

それぞれ641及び1,227 bpに相当する部位から511 bpの配列が欠失したものと一致した。

次に、長期間培養したヒツジ胎児脳由来細胞株OA1からtotal RNA及びゲノムDNAを調製し、同様の実験を行った。5回の継代後に40日間培養したOA1細胞(P5D40)のtotal RNAから合成したfs-cDNAを鋳型としたRT-PCRでは、130及び716 bpのバンドを示したが(Fig. 3B、lanes 1-2)、ゲノムDNAではバンドが検出されなかった(Fig. 3B、lane 5-6)。

以上の結果から、設計したexon-exon junction primerはエクソン結合部位と結合し、構築したRT-PCRでスプライス変異型PrPのmRNAを特異的に検出可能なことが示された。

D. 考察

本研究では遺伝子組換え医薬品等の安全性を確保するため、ウシ血清などの動物由来製造原料を汚染する恐れのあるPrP^{Sc}の新規検出法の確立を目的とし、その基礎研究としてPrPの発現機構に関する研究を行った。

先に、ヒト脳ではGPI欠損型PrPSV mRNAが発現しており、その予想されるアミノ酸配列を認識するモノクローナル抗体を作製し、ヒトグリオブラストーマ細胞株T98Gが蛋白質として産生していることを報告した[Kikuchi *et al.*, *FEBS J.* **275**: 2995-2976 (2008)]。また、昨年度の本研究ではウシ脳及びウシ角膜細胞株BCE C/D-1bがPrPSV mRNAを発現していることを報告した。今年度はヒトPrPSVを認識するモノクローナル抗体作製と同様な手法を用いてPrPSVを認識する抗ペプチド抗体の作製を試み、数度の細胞融合を行ったが、ウシPrPSVを認識する抗体を産生するハイブリドーマを樹立することができなかった。そこで、標準品、マウスの免疫原及び検出用の抗原として用いる組換え蛋白質を調製した。大量に蛋白質を得るために大腸菌を用いた発現系を構築し、抗PrP抗体6H4が認識する組換え端確執の画分を調製した。現在、これらの精製を行っており、来年度はこれらを用いてマウスを免役して新たなモノクローナル抗体の作製を予定している。

プリオン病のバイオマーカーとしてPrPSVを利用することを目的とし、PrPSV mRNAを特異的に検出するexon-exon junction primerを用いたRT-PCR法で血液中の白血球由来total RNAを測定した。測定にはRNAlaterで長期間保存していたウシ血液を検体として用いたところ、わずかながらPrPSV mRNAの発現を確認した。しかし、同じ試料を用いて行った定量RT-PCRでは、その発現量は検出感度以下であった。一般にRNAlater中では、-20°C以下ではRNAは半永久的に安定とされているが、今回用いた試料からは質の良いRNAを得ることができず、定性はできたものの、定量値を出すことができなかった。今後は、新鮮なウシ血液の測定やバフィーコートによる白血球画分の調製を試みて正常なウシ血中を用いたPrPSV mRNAの定量法を確立した上で、プリオン病罹患牛への適応を考えている。

スプライス変異型PrP mRNAの発現は、既にヒト及びウシで確認しているが、本年度はウシと同じ反芻動物のヒツジ脳及びヒツジ培養細胞を対象とし、その発現を確認した。ヒツジに自然発症するプリオン病としスクレイピーが知られており、日本国内でも数例の発症が報告されている。ウシのプリオン病であるBSEは、スクレイピーに罹患したヒツジから動物性飼料を通じて伝達された可能性も指摘されおり、スクレイピーの研究も精力的に行われている。最近、スクレイピー又はBSEに罹患したヒツジの血液を輸血した研究から、43%の確率でスクレイピーが、36%の確率でBSEがそれぞれ伝達されることが報告され、その高い確率から変異型CJD伝達のモデル動物としてヒツジが利用できる可能性が指摘された[Houston *et al.*, *Blood* **112**: 4739-4745 (2008)]。ヒツジを輸血によるCJDやBSEの伝達実験のモデル動物として利用が可能であれば、本研究で報告したexon-exon junction primerを用いたRT-PCR法によるPrPSV mRNAの測定を通じて、それらのバイオマーカーとしての可能性の検証が期待される。

E. 結論

本研究ではウシPrP^{Sc}の新規検出法確立を目的とし、それらに資する基礎研究としてウシPrPSV組換え蛋白質発現系の構築、exon-exon junction primerを用いたRT-PCR法によるウシ血液の測定、ヒツジPrPSV mRNAの解析を行った。これらの結果は、新たなPrP^{Sc}バイオアッセイ系の構築、プリオン病のバイオマーカー測定法開発への寄与が期待できる。

F. 健康危険情報

なし

G. 研究発表

1. 論文発表

Kikuchi Y, Kakeya T, Nakajima O, Sakai A, Ikeda K, Yamaguchi N, Yamazaki T, Tanamoto K, Matsuda H, Sawada J, Takatori K., Hypoxia induces expression of a GPI-anchorless splice variant of the prion protein. *FEBS J.* **275**, 2965-2976 (2008)

2. 学会発表

1. 菊池裕、中島治、山崎壮、手島玲子、棚元憲一、石黒直隆、山口照英：ウシ角膜細胞株BCE C/D-1bが発現するスプライス変異型

GPIアンカー欠損プリオン蛋白質mRNAの解析、2008年プリオン研究会、平成20年8月29-30日、北海道上川郡新得町

2. 菊池裕、遊佐精一、中島治、手島玲子、山口照英：GPIアンカー欠損型プリオン蛋白質産生に関与する低酸素誘導因子の発現解析、第31回日本分子生物学会年会第81回日本生化学会大会合同大会、平成20年12月9-12日、神戸市

H. 知的財産権の出願・登録状況
なし

I. 研究協力者
北海道畜産試験場 基盤研究部 尾上貞雄
国立医薬品食品衛生研究所 代謝生化学部
中島治

研究成果の刊行に関する一覧表

書籍

著者氏名	論文タイトル名	書籍全体の編集者名	書籍名	出版社名	出版地	出版年	ページ
Itoh S., Takakura D., Kawasaki N., Yamaguchi T.	Glycosylation analysis using LC/MS and LC/MSn. Site-specific glycosylation analysis if a glycoprotein.	John Walker	The protein Protocols Hand-book. Third Edition.	Humana Press	U.S.A.	In press	
Kawasaki N., Itoh S., Yamaguchi T.	LC/MS of oligosaccharides	Naoyuki Taniguchi	Glycoscience Lab. Manual.			In press	

雑誌

発表者氏名	論文タイトル名	発表誌名	巻号	ページ	出版年
Kawasaki, N., Itoh, S., Hashii, N., Takakura, D., Qin, Y., Xiaoyu, H., Yamaguchi, Y.	The significance of glycosylation analysis in development of biopharmaceuticals.	Biol. Pharm. Bull			In press
Kawasaki N., Itoh S., Yamaguchi T	LC/MSn for glycoproteome analysis: Glycosylation analysis and peptide sequencing of glycopeptides.	Methods in Molecular Biology	534	1-10	2009
Hashii, N., Kawasaki, N., Itoh, S., Nakajima, Y., Kawanishi, T., Yamaguchi, T.	Alteration of N-glycosylation in the kidney in a mouse model of systemic lupus erythematosus: relative quantification of N-glycans using an isotope-tagging method.	Immunology	126	336-345	2008
Kawasaki, N., Satsuki, I., Hashii, N., Harazono, A., Takakura, T., Yamaguchi, Y.	Mass spectrometry foranalysis of carbohydrate heterogeneity in characterization and evaluation of glycoprotein.	Trends in Glycosci. Glycotech.	20	97-116	2008

Harazono, A., Kawasaki, N., Itoh, S., Hashii, N. Matsuishi-Nakajima,Y., Kawanishi, T., Yamaguch, T.	Simultaneous glycosylation analysis of human serum glycoproteins by high-performance liquid chromatography/tandem mass spectrometry.	J Chromatogr B Analyt Technol Biomed Life Sci.	869	20-30	2008
Itoh S, Hachisuka A, Kawasaki N, Hashii N, Teshima R, Hayakawa T, Kawanishi T, Yamaguchi T.	Glycosylation analysis of IgLON family proteins in rat brain by liquid chromatography and multiple-stage mass spectrometry.	Biochemistry	47	10132-101154	2008
川崎ナナ，石井明子，山口照英	糖鎖と生物薬品	Journal Applied Glycoscience			印刷中
山口照英、石井明子	早期臨床開発段階でのバイオ医薬品の品質・安全性確保	臨床評価			印刷中
Yunoki M, Tanaka H, Urayama T, Hattori S, Ohtani M, Ohkubo Y, Kawabata Y, Miyatake Y, Nanjo A, Iwao E, Morita M, Wilson E, MacLean C, Ikuta K.	Prion removal by nanofiltration under different experimental conditions.	Biologicals	36	27-36	2008
Nishimura T, Sakudo A, Xue G, Ikuta K, Yukawa M, Sugiura K, Onodera T.	Establishment of a new glial cell line from hippocampus of prion protein gene-deficient mice.	Biochem Biophys Res.Commun.	377	1047-1050	2008
Sakudo A, Wu G, Onodera T, Ikuta K.	Octapeptide repeat region of prion protein (PrP) is required at an early stage for production of abnormal prion protein in PrP-deficient neuronal cell line.	Biochem Biophys Res.Commun.	365	164-169	2008
Sakudo A, Taniuchi Y, Kobayashi T, Onodera T, Ikuta K.	Normal cytochrome c oxidase activity in prion protein gene-deficient mice.	Protein Peptide Lett.	15	250-254	2008
Sakudo A, Nakamura I, Tsuji S, Ikuta K.	GPI-anchor-less human prion protein is secreted and glycosylated but lacks SOD activity.	Int J Mol Med.	21	217-222	2008

Sakudo A, Onodera T, Ikuta K	PrPSc level and incubation time in a transgenic mouse model expressing Borna disease virus phosphoprotein after intracerebral prion infection.	Neurosci Lett.	431	81-85	2008
Song C-H, Furuoka H, Kim C-L, Ogino M, Suzuki A, Hasebe R, and Horiuchi, M.	Intraventricular infusion of anti-PrP mAb antagonized PrP^{Sc} accumulation and delayed disease progression in prion-infected mice.	J. Gen. Virol.	89	1533-1544	2008
Muramatsu Y, Sakemi Y, Horiuchi M, Ogawa T, Suzuki K, Kaname da M, Tran Thi Hanh TT, and Tamura Y.	Frequencies of PRNP gene polymorphisms in Vietnamese dairy cattle for potential association with BSE.	Zoonoses Public Health	55	267-273	2008
Takada N, Horiuchi M, Sata T, and Sawada Y.	Evaluation of methods for removing central nervous system tissue contamination from the surface of beef carcasses after splitting.	J. Vet. Med. Sci.	70	1225-1230	2008
Watanabe K, Tachibana M, Tanaka S, Furuoka H, Horiuchi M, Suzuki H, and Watarai M.	Heat shock cognate protein 70 contribute Brucella invasion into trophoblast giant cells that cacuse infectious abortion.	BMC Microbiol.	8	212	2008
Shindoh R, Kim C-L, Song C-H, Hasebe R, and Horiuchi M.	The region approximately between amino acids 81 and 137 of proteinase K-resistant PrP^{Sc} is critical for the infectivity of the Chandler prion strain.	J. Virol.			In press
堀内　基広	プリオンの増殖とその抑制	ウイルス感染症セミナー	10	13-25	2008
Kikuchi Y, Kakeya T, Nakajima O, Sakai A, Ikeda K, Yamaguchi N, Yamazaki T, Tanamoto K, Matsuda H, Sawada J, Takatori K.	Hypoxia induces expression of a GPI-anchorless splice variant of the prion protein.	FEBS J	275	2965-2976	2008

Immunology
The journal of cells, molecules, systems and technologies
British Society for immunology

IMMUNOLOGY ORIGINAL ARTICLE

Alteration of *N*-glycosylation in the kidney in a mouse model of systemic lupus erythematosus: relative quantification of *N*-glycans using an isotope-tagging method

Noritaka Hashii,[1,2] Nana Kawasaki,[1,2] Satsuki Itoh,[1] Yukari Nakajima,[1,2] Toru Kawanishi[1] and Teruhide Yamaguchi[1]

[1]*Division of Biological Chemistry and Biologicals, National Institute of Health Sciences, Setagaya-ku, Tokyo, Japan, and* [2]*Core Research for Evolutional Science and Technology (CREST) of the Japan Science and Technology Agency (JST), Kawaguchi City, Saitama, Japan*

doi:10.1111/j.1365-2567.2008.02898.x
Received 19 March 2008; revised 28 May 2008; accepted 2 June 2008.
Correspondence: N. Kawasaki, Division of Biological Chemistry and Biologicals, National Institute of Health Sciences, 1-18-1 Kamiyouga, Setagaya-ku, Tokyo 158-8501, Japan. Email: nana@nihs.go.jp
Senior author: Teruhide Yamaguchi, email: yamaguch@nihs.go.jp

Summary

Changes in the glycan structures of some glycoproteins have been observed in autoimmune diseases such as systemic lupus erythematosus (SLE) and rheumatoid arthritis. A deficiency of α-mannosidase II, which is associated with branching in *N*-glycans, has been found to induce SLE-like glomerular nephritis in a mouse model. These findings suggest that the alteration of the glycosylation has some link with the development of SLE. An analysis of glycan alteration in the disordered tissues in SLE may lead to the development of improved diagnostic methods and may help to clarify the carbohydrate-related pathogenic mechanism of inflammation in SLE. In this study, a comprehensive and differential analysis of *N*-glycans in kidneys from SLE-model mice and control mice was performed by using the quantitative glycan profiling method that we have developed previously. In this method, a mixture of deuterium-labelled *N*-glycans from the kidneys of SLE-model mice and non-labelled *N*-glycans from kidneys of control mice was analysed by liquid chromatography/mass spectrometry. It was revealed that the low-molecular-mass glycans with simple structures, including agalactobiantennary and paucimannose-type oligosaccharides, markedly increased in the SLE-model mouse. On the other hand, fucosylated and galactosylated complex type glycans with high branching were decreased in the SLE-model mouse. These results suggest that the changes occurring in the *N*-glycan synthesis pathway may cause the aberrant glycosylations on not only specific glycoproteins but also on most of the glycoproteins in the SLE-model mouse. The changes in glycosylation might be involved in autoimmune pathogenesis in the model mouse kidney.

Keywords: isotope-tagging method; liquid chromatography/multiple-stage mass spectrometry; systemic lupus erythematosus

Introduction

Glycosylation is one of the most common post-translational modifications[1,2] and contributes to many biological processes, including protein folding, secretion, embryonic development and cell–cell interactions.[3] Alteration of glycosylation is associated with several diseases, including inflammatory responses and malignancies;[4–6] for instance, significant increases in fucosylation and branching are found in ovarian cancer and lung cancer.[7] Additionally, the carbohydrate structure changes from type I glycans (Galβ1-3GlaNAc) to type II glycans (Galβ1-4GalNAc) in carcinoembryonic antigen in colon cancer.[8] Furthermore, an increase in biantennary oligosaccharides lacking galactose (Gal) was found on immunoglobulin G (IgG) in systemic lupus erythematosus (SLE) and rheumatoid arthritis,[9–11] and agalactoglycans are used for the early diagnosis of rheumatoid arthritis.[12]

Systemic lupus erythematosus is an autoimmune disease characterized as chronic and as a systemic disease, with symptoms such as kidney failure, arthritis and erythema. In addition to the known changes in glycosylation on IgG, there have been several reports on the association between glycosylation and inflammation in SLE and rheumatoid

arthritis.[13–15] A deficiency of α-mannosidase II (αM-II), which is associated with branching in *N*-glycans, has been found to induce human SLE-like glomerular nephritis in a mouse model.[16] Green *et al.* reported that branching structures of *N*-glycan in mammals are involved in protection against immune responses in autoimmune disease pathogenesis.[17] Although there is no direct evidence that alteration of glycosylation is the upstream event in the pathogenesis of SLE, these findings suggest that changes in the glycan structure may be involved in the inflammatory-related autoimmune disorder. Glycosylation analysis may lead to the development of improved diagnostic methods and may help to clarify the carbohydrate-related pathogenic mechanism of inflammation in SLE.

Mass spectrometry (MS) and liquid chromatography/mass spectrometry (LC/MS) are the most prevalent strategies for identifying disease-related glycans in glycomics.[18–20] Aberrant glycosylations in some disease samples have been found by comparing mass spectra or chromatograms between normal and disease samples; however, because of the tremendous heterogeneities of the sugar moiety in glycoprotein as well as the low reproducibility of LC/MS, accurate quantitative analysis is difficult using MS and LC/MS alone. To overcome these problems, we previously developed the stable isotope-tagging method for the quantitative profiling of glycans using 2-aminopyridine (AP).[21] After the glycans are released from sample and the reference glycoproteins are derivatized to pyridyl amino (d_0-PA) glycans and to tetra-deuterium-labelled pyridyl amino (d_4-PA) glycans, respectively, a mixture of both d_0-PA and d_4-PA glycans was subjected to LC/MS, and the levels of individual glycans were calculated from the intensity ratios of d_0-glycan and d_4-glycan molecular ions (Fig. 1a). Recently, alternative isotope-tagging methods using deuterium-labelled compounds, such as 2-aminobenzoic acid its derivatives, and permethylation, have been proposed by other groups.[22–24] All of these studies prove the utility of isotope-tagging methods for the quantitative analysis of glycosylation.

In the present study, we used the isotope-tagging method to analyse changes in *N*-glycosylation in the disordered kidney in an SLE mouse model. We used an MRL/MpJ-lpr/lpr (MRL-lpr) mouse which lacks the Fas antigen gene.[25–27] The MRL-lpr mouse is known to naturally develop SLE-like glomerular nephritis and is widely used in SLE studies. MRL/MpJ-+/+ (MRL-+/+) mice were used as controls.

Materials and methods

Materials

The kidneys of the SLE-model mice (MRL-lpr) and control mice (MRL-+/+) ($n = 3$) were purchased from Japan SLC, Inc. (Hamamatsu, Japan). Thermolysin (EC 3.4.24.27), originating from *Bacillus thermoproteolyticus*

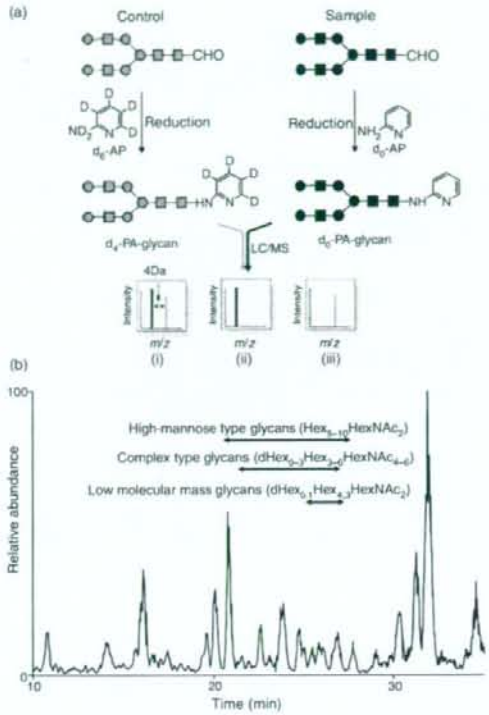

Figure 1. (a) Quantitative glycan profiling using the stable isotope-tagging method and liquid chromatography/mass spectrometry (LC/MS). (i) sample = control, (ii) sample > control, (iii) sample < control. (b) Total ion chromatogram obtained by a single scan (*m/z* 700–2000) of the d_0-glycan and d_4-glycan mixture.

Rokko, was purchased from Daiwa Kasei (Shiga, Japan). Glycopeptidase A (PNGase A) was obtained from Seikagaku Kogyo Corporation (Tokyo, Japan). Non-deuterium-labelled 2-aminopyridine (d_0-AP) and deuterium-labelled 2-aminopyridine (d_6-AP) were purchased from Takara Bio (Otsu, Japan) and Cambridge Isotope Laboratories (Andover, MA), respectively.

Sample preparation

Mouse kidneys were filtered using a cell strainer (70 μm; BD Biosciences, San Jose, CA) and contaminating blood cells in the kidney cells were burst in 140 mM NH_4Cl–Tris buffer (pH 7·2). The surviving kidney cells were washed three times with phosphate-buffered saline containing a mixture of protease inhibitors (Wako, Tokyo, Japan) and dissolved in guanidine–HCl buffer (8 M guanidine–HCl, 0·5 M Tris–HCl, pH 8·6) containing a mixture of protease inhibitors by vortexing at 4°. The protein concentration was measured using a 2-D Quant Kit (GE Healthcare

Bio-Sciences, Uppsala, Sweden). The protein solution (200 μg proteins) was incubated with 40 mM dithiothreitol at 65° for 30 min. Freshly prepared sodium iodoacetate (final concentration, 96 mM) was added to the sample solution, and the mixture was incubated at room temperature for 40 min in the dark. The reaction was stopped by adding cystine (6 mg/ml in 2 M HCl) in an amount equal to the amount of dithiothreitol. The solution containing carboxymethylated proteins was diluted in four times its volume of H_2O, and the mixture was incubated with 0·1 μg of thermolysin at 65° for 1 hr. After terminating the reaction by boiling, the reaction mixture was diluted in four times its volume of 0·2 M acetate buffer. The *N*-linked glycans were released by treatment with PNGase A (1 mU) at 37° for 16 hr and were desalted using an EnviCarb C cartridge (Supelco, Bellefonte, PA).

Labelling of N-glycans with d_0-AP and d_6-AP

Glycans released from the SLE-model mouse cells were incubated in acetic acid (20 μl) with 12·5 M d_0-AP at 90° for 1 hr. Next, 3·3 M borane–dimethylamine complex reducing reagent in acetic acid (20 μl) was added to the solution and the mixture was incubated at 80° for 1 hr. Excess reagent was removed by evaporation, and d_0-PA glycans were desalted using an EnviCarb C cartridge, concentrated in a SpeedVac and reconstituted in 20 μl of 5 mM ammonium acetate (pH 9·6). Glycans released from the control mouse were labelled with d_6-AP in a similar manner. The resulting d_4-PA glycans were combined with d_0-PA glycans, which were prepared from an equal amount of proteins.

On-line liquid chromatography/mass spectrometry

The sample solution (4 μl) was injected into the LC/MS system through a 5-μl capillary loop. The d_0-PA and d_4-PA glycans were separated in a graphitized carbon column (Hypercarb, 150 × 0·2 mm, 5 μm; Thermo Fisher Scientific, Waltham, MA) at a flow rate of 2 μl/min in a Magic 2002 LC system (Michrom Bioresources, Auburn, CA). The mobile phases were 5 mM ammonium acetate containing 2% acetonitrile (pH 9·6, A buffer) and 5 mM ammonium acetate containing 90% acetonitrile (pH 9·6, B buffer). The PA-glycans were eluted with a linear gradient of 5–45% of B buffer for 90 min.

Mass spectrometric analysis of PA glycans was performed using a Fourier transform ion cyclotron resonance/ion trap mass spectrometer (FT-ICR-MS, LTQ-FT; Thermo Fisher Scientific) equipped with a nanoelectrospray ion source (AMR, Tokyo, Japan). For MS, the electrospray voltage was 2·0 kV in the positive ion mode, the capillary temperature was 200°, the collision energy was 25% for MS^n experiment, and the maximum injection times for FT-ICR-MS and MS^n were 1250 and 50 milliseconds, respectively. The resolution of FT-ICR-MS was 50 000, the scan time (*m/z* 700–2000) was approximately 0·2 seconds, dynamic exclusion was 18 seconds, and the isolation width was 3·0 U (range of precursor ions ± 1·5).

Results

Quantitative profiling of kidney oligosaccharides in the SLE-model mouse

The recovery of oligosaccharides from whole tissues and cells is generally low because of the insolubility of the membrane fraction and possible degradation of the glycans. To improve the recovery of *N*-glycans from kidney cells, whole cells were dissolved in guanidine hydrochloride solution, and all proteins, including membrane proteins, were digested into peptides and glycopeptides with thermolysin. The *N*-glycans were then released from the glycopeptides with PNGase A, which is capable of liberating *N*-linked oligosaccharides even at the N- and/or C-terminals of peptides. The *N*-linked oligosaccharides from the SLE-model mice and control mice were labelled with d_0-AP and d_6-AP, respectively. The mixture of labelled glycans derived from an equal amount of proteins was subjected to quantitative glycan profiling using LC/MS^n.

Figure 1(b) shows the total ion chromatogram obtained by a single mass scan (*m/z* 700–2000) of the glycan mixture in the positive ion mode. Although the MS data contain many MS spectra derived from contaminating low-molecular-weight peptides, the MS/MS spectra of oligosaccharides could be sorted based on the existence of carbohydrate-distinctive ions, such as $HexHexNAc^+$ (*m/z* 366) and $Hex(dHex)HexNAc^+$ (*m/z* 512). The monosaccharide compositions of the precursor ions were calculated from accurate *m/z* values acquired by FT-ICR-MS. Oligosaccharides found at 25–27 min were assigned to low-molecular-mass glycans consisting of $dHex_{0,1}Hex_{4,3}HexNAc_2$ (dHex, deoxyhexose; Hex, hexose; HexNAc, *N*-acetylhexosamine). High-mannose-type glycans, which consist of $Hex_{5-10}HexNAc_2$, were located at 20–28 min; complex-type glycans ($dHex_{0-3}Hex_{3-6}HexNAc_{4-6}$) were found at 21–27 min. Figure 2(a) shows the relative intensities of the molecular ions of *N*-glycans in the SLE-model mouse, which may correspond roughly to the levels of individual *N*-glycans. More than half of all glycans were complex-type oligosaccharides, and the most prominent glycan was $dHex_3Hex_5HexNAc_5$. Man-9 ($Hex_9HexNAc_2$) was the second most common oligosaccharide. Nearly one-quarter of the glycans were low-molecular-mass glycans, and $dHex_1Hex_2HexNAc_2$ was the third most abundant glycan in the SLE-model mouse. The rate of percentage change in individual glycans between the SLE-model mice and control mice was calculated from the intensity ratio of d_0-glycan and d_4-glycan

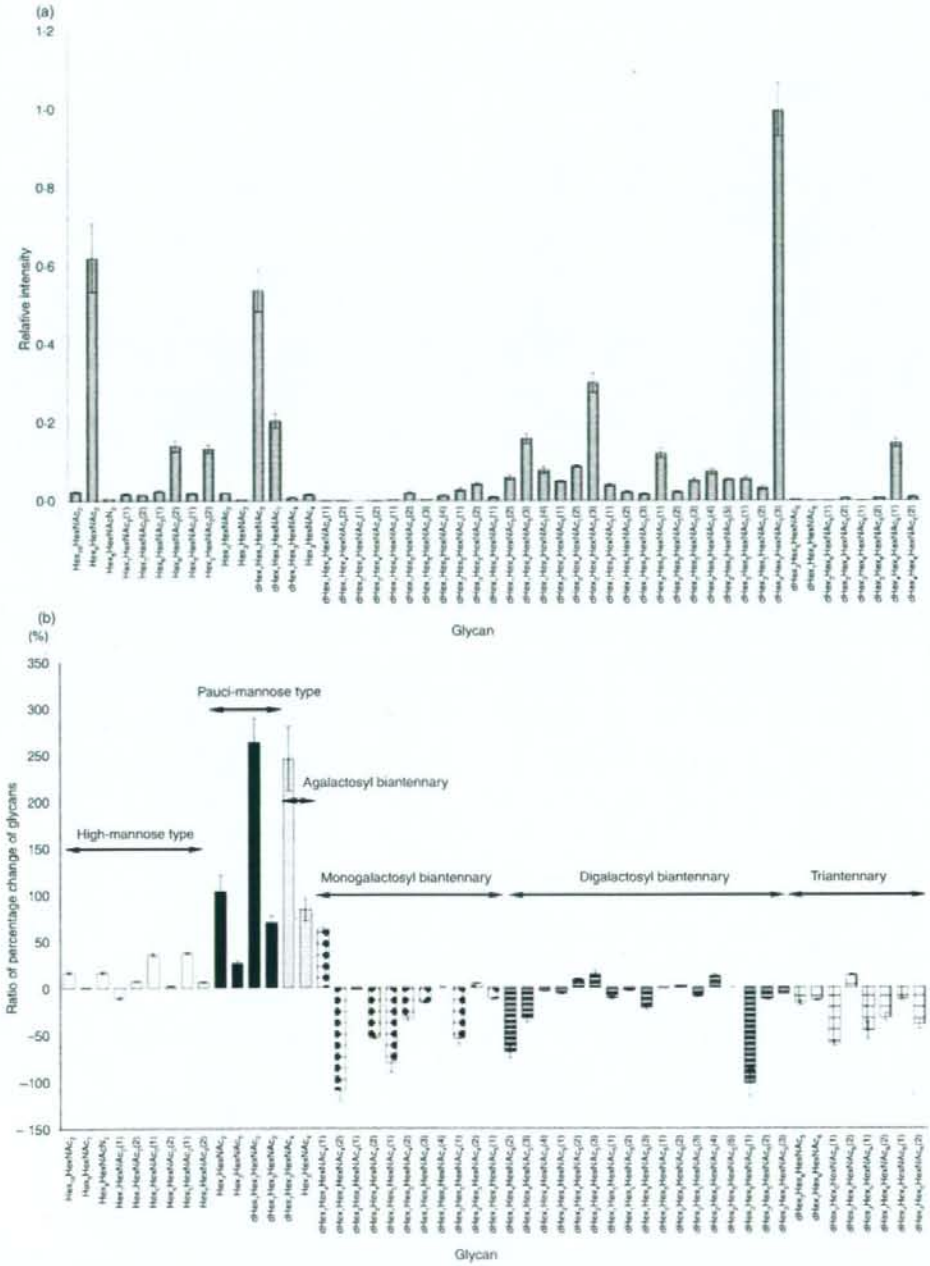

Figure 2. (a) Relative intensities of the molecular ions of d_0-pyridyl amino (PA) glycans from the systemic lupus erythematosus (SLE) model mouse. The intensity of the most intense ion ($[M + 2H]^{2+}$ of d_4-PA $dHex_3Hex_3HexNAc_3(3)$, *m/z* 1180·97) was taken as 1·0. (b) Rate of percentage change of d_0/d_4-glycans. Each value is the average of three biological repeats. Error bars correspond to the standard deviation. The numbers in parentheses show the isomers.

molecular ions (Fig. 2b). The significant changes found in many glycans are described below.

Increased oligosaccharides in the SLE-model mouse

Figure 3(a,b) show the mass and MS/MS spectra of the most increased glycan, which showed a notable increase in the SLE-model mouse. Based on *m/z* values of molecular ions and differences of 1·00 U in *m/z* values among monoisotopic ions, the intense ion (*m/z* 973·40) and its neighbour ion (*m/z* 977·43) were assigned to $[M+H]^+$ of d_0-PA $dHex_1Hex_2HexNAc_2$, and d_4-PA $dHex_1Hex_2HexNAc_2$, respectively (Fig. 3a). The intensity ratio of these ions suggested that the level of $dHex_1Hex_2HexNAc_2$ increased 3·6-fold in the SLE-model mouse. The structure of this oligosaccharide was estimated to be a core-fucosylated trimannosyl core lacking a Man residue from the successive cleavages of Man (Y_3: *m/z* 815), Man (Y_2: *m/z* 653), GlcNAc (Y_1: *m/z* 450) and Fuc ($Y_{1/1'}$: *m/z* 304) (inset in Fig. 3b). Such a defective *N*-glycan is known as a paucimannose-type glycan, and is rarely found in vertebrates. All paucimannose-type glycans, such as $dHex_1Hex_3HexNAc_2$ (a core-fucosylated trimannosyl core) and $Hex_3HexNAc_2$ (a non-fucosylated trimannosyl core) were increased in the SLE-model mouse. Furthermore, a two-fold increase was found in $Hex_4HexNAc_2$ (Man-4).

Figure 4 shows the molecular ratios of individual *N*-glycans between the SLE-model mice and control mice. A remarkable increase (3·5-fold) was also found in $dHex_1Hex_3HexNAc_4$, which is assigned to a core-fucosylated biantennary oligosaccharide lacking two non-reducing terminal Gal residues; its non-fucosylated form ($Hex_3HexNAc_4$) was also increased 1·8-fold in the SLE-model mouse. In other complex-type glycans, $dHex_1Hex_4HexNAc_4$ (1), which is assigned to a biantennary oligosaccharide lacking one molecule of Gal, increased 1·6-fold. Interestingly, a significant decrease was found in $dHex_1Hex_4HexNAc_4$ (2), a positional isomer of $dHex_1Hex_4HexNAc_4$ (1); this might have been caused by galactosylation on either GlcNAc-Manα1–3 or GlcNAc-Manα1–6. In contrast, no change was found between fucosylated and non-fucosylated oligosaccharides, nor between bisected and non-bisected oligosaccharides.

A significant increase was found in some high-mannose-type oligosaccharides, such as $Hex_5HexNAc_2$ (Man-5; + 137%) and $Hex_6HexNAc_2$ (1) (Man-6; + 136%), while $Hex_7HexNAc_2$ (1,2) (Man-7) and a positional isomer of $Hex_6HexNAc_2$ (1) [$Hex_6HexNAc_2$ (2)] remained unchanged in the SLE-model mouse. A slight increase was found in $Hex_8HexNAc_2$ (Man-8; + 116%) and $Hex_{10}HexNAc_2$ (possibly assigned to Man-9 plus Glc; + 116%).

Decreased oligosaccharides in the SLE-model mouse

The mass spectrum of the most decreased glycan is shown in Fig. 5(a). Based on differences of 0·5 U in *m/z* values among monoisotopic ions, molecular ions at *m/z* 1180·97

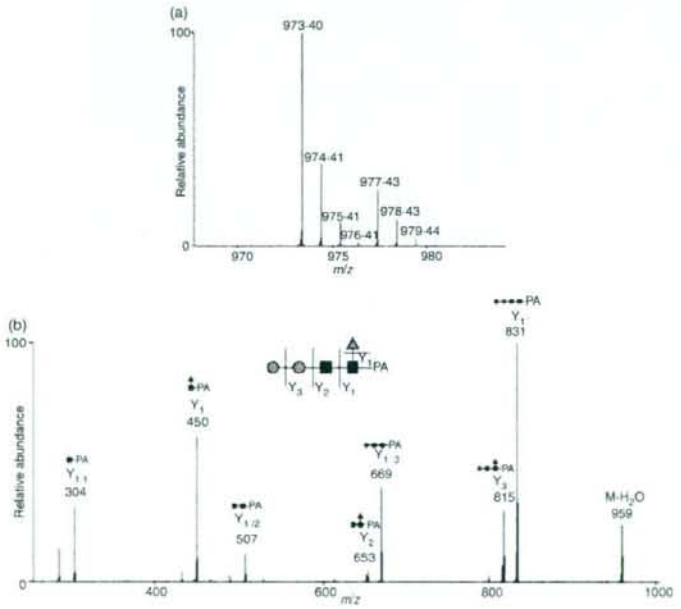

Figure 3. Mass (a) and mass spectrometry (MS)/MS (b) spectra of the most increased glycan ($dHex_1Hex_2HexNAc_2$). Precursor ion, *m/z* 973·4; grey circle, mannose; grey triangle, fucose; black square, *N*-acetylglucosamine.

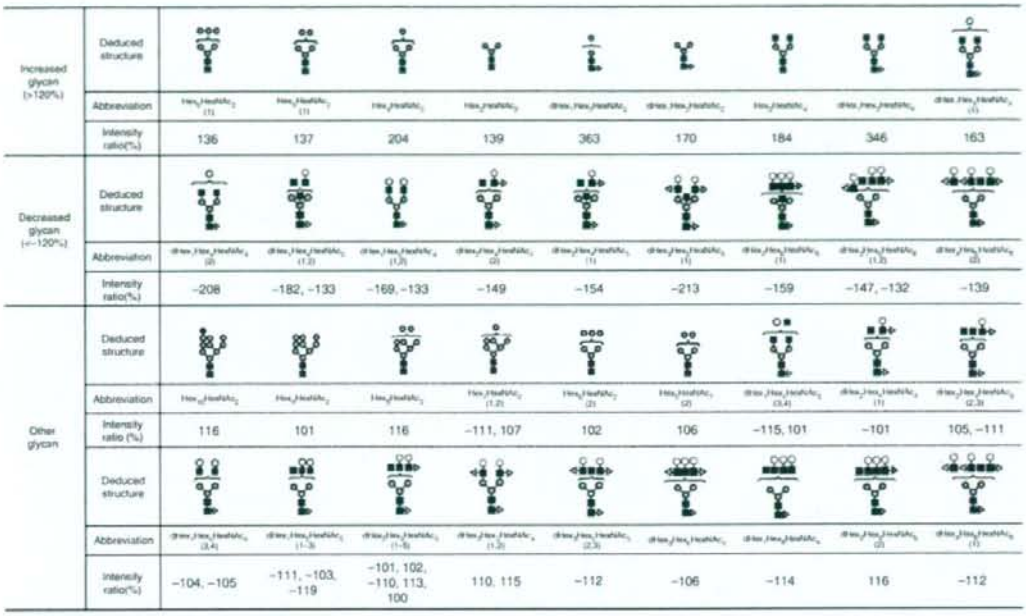

Figure 4. Summary of quantitative analysis of the systemic lupus erythematosus (SLE) model mouse against control mice. Values of relative ratios are the averages of three biological repeats. Grey circle, mannose; white circle, galactose; grey triangle, fucose; black square, *N*-acetylglucosamine.

and 1182·98 are estimated to be $[M + 2H]^{2+}$ of d_0-PA and d_4-PA $dHex_3Hex_5HexNAc_5$ (1), respectively. The intensity ratio of $d_0 : d_4$ glycans suggests that this glycan in the SLE-model mouse was decreased to 47% of the amount found in the control mouse. Figure 5(b) shows the MS^{2-4} spectra of d_0-PA $dHex_3Hex_5HexNAc_5$ (1) (precursor ion, *m/z* 1180·97). The fragment ion at *m/z* 512 in MS/MS (i) and MS/MS/MS (ii) spectra, which corresponds to $dHex_1Hex_1HexNAc_1^+$, suggests the attachment of two Lewis motifs on the side chains of the glycan. The presence of $dHex_1HexNAc_1PA^+$ (*m/z* 446) and $dHex_1Hex_1HexNAc_3PA^+$ (*m/z* 1015) reveals the linkages of a core fucose and a bisecting GlcNAc. Based on these fragments, this decreased glycan is estimated to be a Lewis-motif-modified, core-fucosylated and bisected biantennary oligosaccharide (inset in Fig. 5).

As shown in Figs 2(b) and 4, oligosaccharides lacking one molecule of Gal with and without bisecting GlcNAc [$dHex_1Hex_4HexNAc_4$ (2) and $dHex_1Hex_4HexNAc_5$ (1)] were decreased to 48% and 55%, respectively. A significant decrease was also found in other monogalactobiantennary oligosaccharides, such as $dHex_2Hex_4HexNAc_4$ (2) (a Lewis-motif-modified, core-fucosylated monogalacto-biantennary) and $dHex_2Hex_4HexNAc_5$ (1) (a Lewis-motif-modified core-fucosylated and bisected monogalacto-biantennary).

The oligosaccharides, non-reducing ends of which are fully galactosylated, were decreased in the SLE-model mouse. For example, monofucosyl biantennary $dHex_1Hex_5HexNAc_4$ (1) and (2) were decreased 59% and 75%, respectively. The di-, tri- and tetra-fucosylated oligosaccharides, $dHex_2Hex_6HexNAc_6$ (1), $dHex_3Hex_6HexNAc_6$ (1,2) and $dHex_4Hex_6HexNAc_6$ (1,2), which were estimated to be tri- and tetraantennary forms, were also significantly decreased. These results show that oligosaccharides with a complicated structure, such as high branching oligosaccharides and di- and tri-fucosylated oligosaccharides, were decreased in the SLE-model mouse.

Discussion

Using the isotope-tagging method, we demonstrated aberrant *N*-glycosylation on the kidney proteins of a SLE-model mouse. We found increases in low-molecular-mass glycans with simple structures, including paucimannose-type glycans, agalacto-biantennary oligosaccharides, Man-5 and Man-6, and decreases in glycans which have a complicated and diverse structure, such as digalacto-biantennary oligosaccharides and highly fucosylated glycans (Fig. 4). An increase in agalacto-biantennary oligosaccharides on IgG has been reported in the sera of patients with autoimmune diseases, including SLE, rheumatoid arthritis and IgA

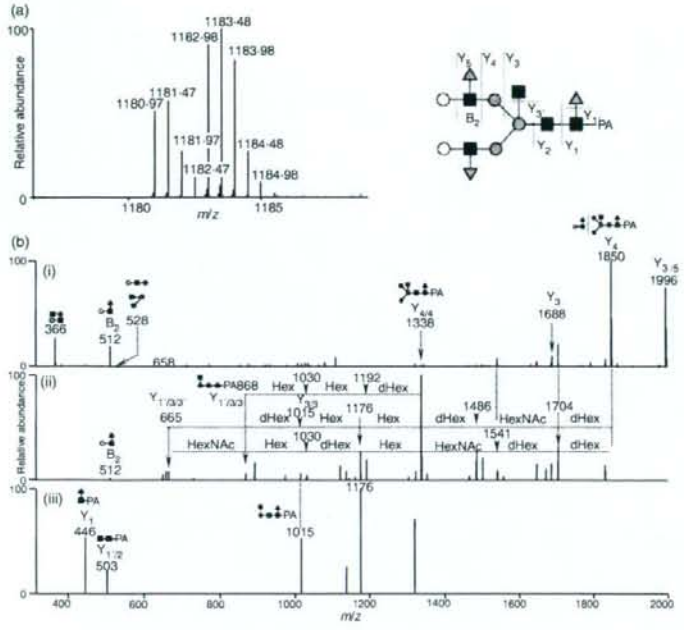

Figure 5. (a) Mass spectrum of the most decreased glycan [$dHex_3Hex_5HexNAc_5$ (1)]; (b-i) Mass spectrometry (MS)/MS spectrum of *m/z* 1181·0; (b-ii) MS/MS/MS spectrum of *m/z* 1849·7; (b-iii) MS/MS/MS/MS spectrum of *m/z* 1338·3. Grey circle, mannose; white circle, galactose; grey triangle, fucose; black square, *N*-acetylglucosamine; dHex, deoxyhexose (fucose); Hex, hexose (mannose and galactose); HN, *N*-acetylhexosamine (*N*-acetylglucosamine).

nephropathy.[9,11,28] The present findings show that abnormal glycosylation occurs not only in IgG in serum but also in several glycoproteins in the SLE-model mouse kidney.

Figure 6 shows the biosynthesis pathway of *N*-linked oligosaccharides in mammalian cells. Man-9, a product in the early stage of the pathway, is processed to Man-5 in the endoplasmic reticulum, and a GlcNAc and Fuc are added to Man-5 in the Golgi apparatus. After the removal of two Man residues by αM-II, GlcNAc, Gal and Fuc are further added to oligosaccharides by several glycosyltransferases. There have been a few reports on paucimannose-type oligosaccharides in vertebrates;[29] however, these glycans are common oligosaccharides in other multicellular organisms such as insects and *Caenorhabditis elegans*.[30,31] The membrane protease β-*N*-acetylglucosaminidase is thought to mediate the synthesis of paucimannose-type oligosaccharides.[32] Based on core fucosylation on some paucimannose-type oligosaccharides, it was deduced that β-*N*-acetylglucosaminidase might act on glycan synthesis after *N*-acetylglucosaminyltransferase I, core fucosyltransferase and αM-II.[32] The synthesis of paucimannose-type oligosaccharides may be involved in the suppression of growing diversity and complexity of glycan structures.

We found a number of changes in the levels of monogalacto-biantennary oligosaccharides in the SLE mouse. Galactosylation to agalacto-biantennary oligosaccharides is mediated by β-1,4-galactosyltransferase

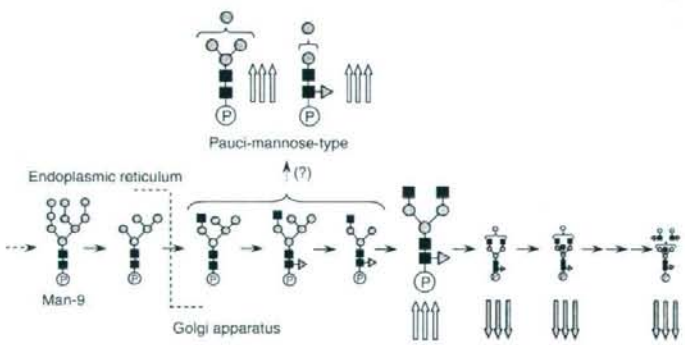

Figure 6. Biosynthesis pathway of *N*-linked oligosaccharides in mammalian cells. Triple up-arrow, increases of more than +2·0; triple down-arrow, decreases of not more than −2·0. Grey circle, mannose; white circle, galactose; grey triangle, fucose; black square, *N*-acetylglucosamine. 'P' is protein portion.

(β-1,4-GalTase).[33] Previous studies suggested that translational repression of β-1,4-GalTase in lymphocytes is associated with an increase in agalacto-oligosaccharides on IgG in the serum of the MRL-lpr mouse.[34] Although the activity of β-1,4-GalTase remains unknown in the SLE-model mouse, the increase in agalacto forms and the decrease in digalacto forms imply changes in β-1,4-GalTase activity. The present results suggest a decrease in diverse and complex glycans, which are synthesized at a late stage in the *N*-glycan synthesis pathway, and an increase in the simple glycans appearing at an early stage in the SLE-model mouse.

The activation of complements is involved in glomerular nephritis of SLE.[35–37] The complements are activated through three pathways: a classical pathway, an alternative pathway and a lectin pathway. In the classical pathway, a binding of C1q to an immune complex triggers the activation of C1r and C1s. Activated C1s cleaves C4 and C2, generating C3 convertase (C4b2a), which generates C3b. The complement component subsequently produces C5b-9 complex, which leads to an inflammatory response on host tissues.[38–41] The excess deposition of immune complexes followed by a sustained immune response triggers tissue disorders, including lupus nephritis.[42–45] In the lectin pathway, mannose-binding lectin (MBL) is associated with the activation of complements. Two forms of MBL (MBL-A and MBL-C) are present in complexes with MBL-associated serine proteases (MASPs) in mice. The MASPs are activated by binding MBL to Man or GlcNAc on the surface of the antigen in a calcium-dependent manner.[46–49] Like C1s in the classical pathway, activated MASPs cleave C4 and C2.[50,51] In lupus nephritis, MBL-A and MBL-C in the immune complex bind to GlcNAc residues at the reducing ends of agalacto-biantennary oligosaccharides in IgG,[52] and subsequently activate the complements.[53,54] In αM-II-deficient mice, which suffer from SLE-like syndromes including kidney disorders, the majority of glycans are hybrid-type oligosaccharides because of the failure of Man trimming by the lack of αM-II.[16] Green *et al.* concluded that MBL recognized Manα1–3 and Manα1–6 linkages in hybrid-type oligosaccharides,[17] and glycans lacking normal side chains, including agalacto-biantennary oligosaccharides, might be involved in the aberrant immune response in autoimmune diseases. Paucimannose glycans, which contain exposed Manα1–3 or Manα1–6 linkages, may be recognized as ligand carbohydrates by MBL. Our present finding, an increase in paucimannose oligosaccharides and agalacto forms, might result from an alteration of the biosynthesis pathway of *N*-glycans. The alterations may cause the aberrant glycosylations on most of the glycoproteins rather than some glycoproteins in the SLE-model mouse. The changes in glycosylation might be involved in an autoimmune pathogenesis in the SLE-model mouse kidney.

The continuous production of aberrant antibodies that react with components from self-tissue and accumulation in the immune complex are thought to promote tissue damage in autoimmune disease.[55,56] The mechanism of localized accumulation in the immune complex in some tissues remains unknown in SLE. We found an increase in glycans that may bind to MBL and subsequently promote complement activation via the lectin pathway in the mouse kidney. Our present results suggest that an aberrant *N*-glycan synthesis pathway as well as an abnormal immune system may be involved in the damage caused by glomerular nephritis in the SLE-model mouse.

Acknowledgements

This study was supported in part by a Grant-in-Aid from the Ministry of Health, Labor, and Welfare, and Core Research for the Evolutional Science and Technology Program (CREST), Japan Science and Technology Corp (JST).

References

1 Dwek RA. Glycobiology: toward understanding the function of sugars. *Chem Rev* 1996; **96**:683–720.
2 Helenius A, Aebi M. Intracellular functions of N-linked glycans. *Science* 2001; **291**:2364–9.
3 Zak I, Lewandowska E, Gnyp W. Selectin glycoprotein ligands. *Acta Biochim Pol* 2000; **47**:393–412.
4 Axford JS. Glycosylation and rheumatic disease. *Biochim Biophys Acta* 1999; **1455**:219–29.
5 Feizi T, Gooi HC, Childs RA, Picard JK, Uemura K, Loomes LM, Thorpe SJ, Hounsell EF. Tumour-associated and differentiation antigens on the carbohydrate moieties of mucin-type glycoproteins. *Biochem Soc Trans* 1984; **12**:591–6.
6 Kannagi R, Izawa M, Koike T, Miyazaki K, Kimura N. Carbohydrate-mediated cell adhesion in cancer metastasis and angiogenesis. *Cancer Sci* 2004; **95**:377–84.
7 Goodarzi MT, Turner GA. Decreased branching, increased fucosylation and changed sialylation of alpha-1-proteinase inhibitor in breast and ovarian cancer. *Clin Chim Acta* 1995; **236**:161–71.
8 Yamashita K, Fukushima K, Sakiyama T, Murata F, Kuroki M, Matsuoka Y. Expression of Sia alpha 2→6Gal beta 1→4GlcNAc residues on sugar chains of glycoproteins including carcinoembryonic antigens in human colon adenocarcinoma: applications of *Trichosanthes japonica* agglutinin I for early diagnosis. *Cancer Res* 1995; **55**:1675–9.
9 Tomana M, Schrohenloher RE, Reveille JD, Arnett FC, Koopman WJ. Abnormal galactosylation of serum IgG in patients with systemic lupus erythematosus and members of families with high frequency of autoimmune diseases. *Rheumatol Int* 1992; **12**:191–4.
10 Mizuochi T, Hamako J, Nose M, Titani K. Structural changes in the oligosaccharide chains of IgG in autoimmune MRL/Mp-lpr/lpr mice. *J Immunol* 1990; **145**:1794–8.
11 Arnold JN, Wormald MR, Sim RB, Rudd PM, Dwek RA. The impact of glycosylation on the biological function and structure